Optimal Power Flow Modelling and Analysis of Hybrid AC-DC Grids with Offshore Wind Power Plant

Dhua, Debasish; Huang, Shaojun; Wu, Qiuwei

Published in:
Energy Procedia

Link to article, DOI:
10.1016/j.egypro.2017.11.076

Publication date:
2017

Document Version
Publisher's PDF, also known as Version of record

Available online at www.sciencedirect.com

ScienceDirect

Energy Procedia 141 (2017) 572–579

Energy Procedia

www.elsevier.com/locate/procedia

4th International Conference on Power and Energy Systems Engineering, CPESE 2017, 25-29 September 2017, Berlin, Germany

Optimal Power Flow Modelling and Analysis of Hybrid AC-DC Grids with Offshore Wind Power Plant

Debasish Dhua[a], Shaojun Huang[*a], Qiuwei Wu[a]

[a]*Centre for Electric Power and Energy, Department of Electrical Engineering, Technical University of Denmark, Elektrovej 325, 2800 Kgs. Lyngby, Denmark*

Abstract

In order to develop renewables based energy systems, the installation of the offshore wind power plants (WPPs) is globally encouraged. However, wind power generation is intermittent and uncertain. An accurate modelling and evaluation reduces investment and provide better operation. Hence, it is essential to develop a suitable model and apply optimization algorithms for different application scenarios. The objective of this work is to develop a generalized model and evaluate the Optimal Power Flow (OPF) solutions in a hybrid AC/DC system including HVDC (LCC based) and offshore WPP (VSC based). This paper also shows the significance and impact of control parameters in OPF applications. An integrated hybrid power system network is adopted in this paper and OPF techniques are applied on it by considering the impact of different control parameters. In addition to the impact of the control variables, the wind power production level also plays a major role in a hybrid system on transmission loss evaluation. The developed model is tested in Low, Medium and High wind power production levels to determine the objective function of the OPF solution. MATLAB Optimization Toolbox and MATLAB script are used to develop the model for the case studies.

Peer-review under responsibility of the scientific committee of the 4th International Conference on Power and Energy Systems Engineering.

Keywords: Hybrid AC-DC System; Load Flow; Newton-Raphson Method; Offshore Wind Power Plant; OPF; Transmission Loss.

1. Introduction

Among multiple renewable energy sources (RESs), Offshore Wind Technology (OWT) is the flagship technology to drive the growth of sustainable energy technologies over the world. It provides the highest load hours amongst all RESs with more than 4800 full load hours per year and more than 8000 operation hours, which is

* Corresponding author. Tel.: +45 45 25 34 95.
E-mail address: shuang@elektro.dtu.dk.

1876-6102
Peer-review under responsibility of the scientific committee of the 4th International Conference on Power and Energy Systems Engineering.
10.1016/j.egypro.2017.11.076

equivalent to 340 days of production [1]. OWT is the key solution for existing and future EU energy market to meet the 2030 energy target [2-3]. The interconnection of North-sea countries though OWT and High Voltage DC (HVDC) transmission is the backbone of future EU supergrid [1], [4]. The studies and innovations on the OWT-hybrid grid system can be broadly classified into two categories: a) voltage source converter multi-terminal DC (VSC-MTDC) power flow control and protections, and b) Mathematical modelling and optimization power flow (OPF) studies [5]. A large proportion of the relevant publications address the existing technical challenges in OWT including over/under voltage issues, wind curtailment and HVDC transmission protection and possible solutions [6-21]. Mathematical modelling of load flow studies is covered by another set of publications. MATLAB, GAMS, MATACDC, MATPOWER are the popular simulation tools used for optimization studies [7], [13]. Although multiple literatures exist that cover the OPF method in a hybrid HV transmission system [5], [11], there is few about the generalized and detailed algorithm dedicated to hybrid AC/DC systems, e.g. considering both firing angles of LCC based HVDC transmission lines and VSC based OWT. The objective of this paper is to develop a generalized OPF model of a hybrid grid and OWT. It is designed to minimize the transmission loss in the entire network so as to operate the entire grid efficiently and economically. Moreover, the developed OPF model is applied in a hybrid system under different wind power generation capabilities to estimate the objective function which is minimization of transmission loss in this case.

The rest of the paper is organized as follows. Section 2 lists the load flow constraints. Section 3 introduces different objective functions for the OPF analysis. Section 4 presents the Optimal Power Flow results and discussion. Section 5 concludes this work with future extension possibilities.

2. Load flow constraints modelling

In a hybrid multi-terminal HVDC network, there are three sets of constraints existing in order to control the overall power flow. The constraints can be expressed in terms of a set of power flow equalities and inequalities as, I) Converter power conversion constraints, II) DC power flow constraints, III) AC power flow constraints.

2.1. Converter power conversion constraints

From the load flow point of view, there is a generalized configuration that can be applied to both AC and DC system at the junction point, since the converter can be treated as a power injector at either point. For an AC/DC converter the power flow equation can be expressed as below,

$$P_{AC,i} + P_{DC,i} + P_{loss,i} = 0, \tag{1}$$

where, $P_{AC,i}$ represents the active power flow into the AC system, $P_{DC,i}$ represents active power flow into the DC system and $P_{loss,i}$ is the active power loss inside *i-th* converter. Similar interactive power flow equation as (1) is not applicable for reactive power flow, since the HVDC line decouples the reactive power transmission through it and is separately controlled at the two ends of the HVDC line by using the power electronic interfaces. Hence, the reactive power flow constraints can only be developed for the AC segment analysis. The AC/DC interaction can be elaborated in two segments as shown in Fig 1.

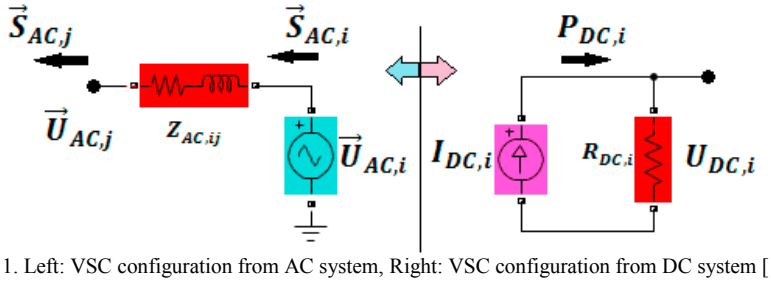

Fig. 1. Left: VSC configuration from AC system, Right: VSC configuration from DC system [16]

Observing from the AC power system, *i-th* Voltage Source Converter can be seen as a voltage source with generating voltage $\vec{U}_{AC,i}$ and injecting power $\vec{S}_{AC,i} = P_{AC,i} + jQ_{AC,i}$ to *j-th* nodal point, expressed in (2) and (3) [17]. In (2) and (3), $G_{AC,ij} + jB_{AC,ij} = 1/Z_{AC,ij}$ is per phase AC Transmission line admittance as seen from the AC side between the *i-th* and *j-th* node.

$$P_{AC,i} = U_{AC,i}^2 G_{AC,ij} - U_{AC,i}U_{AC,j}\left(G_{AC,ij}\cos\left(\delta_{AC,i} - \delta_{AC,j}\right) + B_{AC,ij}\sin\left(\delta_{AC,i} - \delta_{AC,j}\right)\right) \tag{2}$$

$$Q_{AC,i} = -U_{AC,i}^2 B_{AC,ij} - U_{AC,i}U_{AC,j}\left(G_{AC,ij}\sin\left(\delta_{AC,i} - \delta_{AC,j}\right) - B_{AC,ij}\cos\left(\delta_{AC,i} - \delta_{AC,j}\right)\right) \tag{3}$$

$$P_{AC,i} - P_{AC,j} - P_{loss,AC,ij} = 0 \tag{4}$$

$$Q_{AC,i} - Q_{AC,j} = 0 \tag{5}$$

2.2. DC power flow constraints

As indicated in Fig 1, the Converter system can be considered as a constant current source from the DC system with an injection current $I_{DC,i}$ by *i-th* converter into the DC system. $Y_{DC,ij}$ is the DC bus admittance between *i-th* and *j-th* DC node. Hence, the total active power injected by *i-th* node into the DC system can be expressed as (6).

$$I_{DC,i} = \sum_{j=1}^{n_{DC}} Y_{DC,ij}\left(U_{DC,i} - U_{DC,j}\right) \tag{6}$$

$$P_{DC,i} = U_{DC,i}I_{DC} + P_{loss,DC,ij} \tag{7}$$

The offshore wind turbines (WTs) produce AC power which then converted to high voltage DC power and transmitted through the long distance submarine cable to the onshore transformer. In further, the transmitted DC power is inverted to AC power by the onshore converter system and fed into the main land AC grid. Hence, the two terminal DC link needs to be further analyzed as in [18].

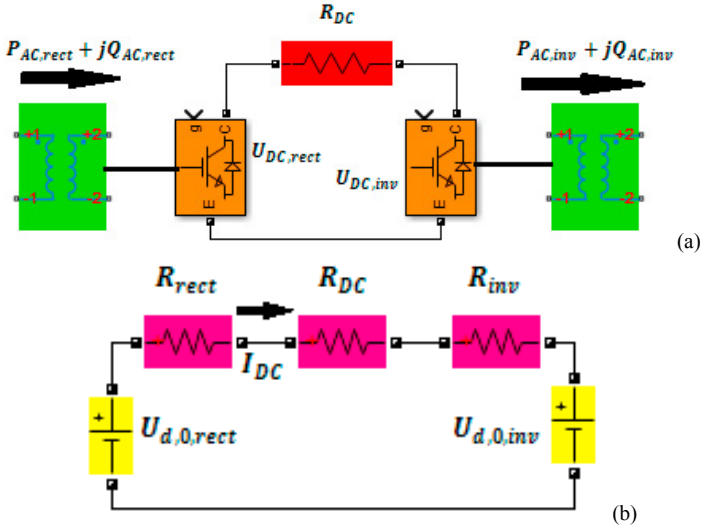

Fig 2 a). Two terminal model of HVDC transmission link, b) Close loop circuit representation of two-terminal DC link

To analyze the steady state converter operation, the following assumptions can be made for further detailing of the load flow constraints, a) the AC terminal voltages are perfectly balanced and sinusoidal, b) the rectifier and inverter are capable of ideal AC/DC conversion and c) DC current does not contain any AC component. If the AC to DC rectifier terminal is denoted by 'rect' and DC to AC inverter terminal is denoted by 'inv', the Kirchhoff's laws can be separately expressed for Rectifier and Inverter Terminals.

Rectifier and Inverter Equations

$$U_{d,0,rect} = kn_{rect}U_{AC,rect} \tag{8}$$

$$U_{d,rect} = U_{d,0.rect}cos\alpha_{rect} - R_rI_{d,rect} \tag{9}$$

$$P_{rect} = U_{d,rect}I_{d,rect} \tag{10}$$

$$Q_{rect} = U_{d,rect}I_{d,rect}\tan\varphi_{rect} \tag{11}$$

$$U_{d,0,inv} = kn_{inv}U_{AC,inv} \tag{12}$$

$$U_{d,inv} = U_{d,0.inv}cos\gamma_{inv} - R_{inv}I_{d,inv} \tag{13}$$

$$P_{inv} = U_{d,inv}I_{d,inv} \tag{14}$$

$$Q_{inv} = U_{d,inv}I_{d,inv}\tan\varphi_{inv} \tag{15}$$

where $U_{d,0,rect}$, $U_{d,0,inv}$ are the ideal no-load DC voltage after conversion of the per phase AC voltage U_{rect} at the rectifier terminal and U_{inv} at the inverter terminal respectively, k = $3\sqrt{2}/\pi$ is the AC/DC conversion factor, α_{rect} , γ_{inv} are the rectifier and inverter firing angle respectively. Although firing angles are normally for LCC based HVDC, they are employed here for describing the voltage magnitude relation between the AC and DC side of the VSC converters in order to have a generalized form for both technologies (LCC and VSC). R_{rect}, R_{inv} represent the equivalent commutating resistance of the rectifier and inverter respectively. Since, the losses at the transformers and converters are neglected hence, $P_{rect} = P_{AC,rect}$ & $Q_{rect} = Q_{AC,rect}$ and $P_{inv} = P_{AC,inv}$ & $Q_{inv} = Q_{AC,inv}$. The active power flow direction depends on the direction of current I_{DC} flowing in the DC network, which is decided by the voltage levels at the two terminals of the DC network. The reactive power is either injected into the AC network or absorbed from the AC network at the terminals since there is no reactive power transmission through the DC network. φ_{rect}, φ_{inv} are the power factor at the rectifier and inverter terminals respectively connected to AC terminal.

Line equation

The line current through the DC link between the rectifier and inverter is expressed as (16). $I_{DC} = I_{DC,rect} = I_{DC,inv}$ and R_{DC} is the DC line resistance.

$$I_{DC} = \frac{U_{d,rect} - U_{d,inv}}{R_{DC}} \tag{16}$$

Converter constraints

The converter loss of *i-th* converter as indicated in (1) can be expressed as a function of converter current.

$$P_{loss,i} = a_i + b_iI_{C,i} + c_iI_{C,i}^2 \tag{17}$$

where a_i, b_i, c_i are the VSC loss parameters, which depends on the specific power electronic component used in the Converter and $I_{Conv,i} = \sqrt{P_{Conv,i} + Q_{Conv,i}}/U_{Conv,i}$. Some more converter operating constraints for *i-th* converter (as shown in Figure 2) can be listed in following inequalities; where $I_{Conv,i,max}$ is the maximum allowable converter current limit and $U_{DC,i,min}$, $U_{DC,i,max}$ are the minimum and maximum applied voltage across the converter, respectively. The maximum current carrying capacity of submarine cable is $I_{DC,max}$.

$$-I_{Conv,i,max} \leq I_{Conv,i} \leq I_{Conv,i,max} \tag{18}$$

$$U_{DC,i,min} \leq U_{DC,i} \leq U_{DC,i,max} \tag{19}$$

$$-I_{DC,max} \leq I_{DC,i} \leq I_{DC,max} \tag{20}$$

2.3. AC power flow constraints

In order to determine the Optimal Power Flow subject to maximizing/minimizing a certain objective function, the following non-linear equalities are valid.

$$\sum_{k \in i} P_{Gk} - \sum_{k \in i} P_{Lk} - \sum_{k \in i} P_{Conv,k} = \sum_{j=1}^{n_{AC}} U_{AC,i} U_{AC,j} \left[G_{AC,ij} \cos\left(\delta_{AC,ij}\right) + B_{AC,ij} \sin\left(\delta_{AC,ij}\right) \right] \tag{21}$$

$$\sum_{k \in i} Q_{Gk} - \sum_{k \in i} Q_{Lk} - \sum_{k \in i} Q_{Conv,k} = \sum_{j=1}^{n_{AC}} U_{AC,i} U_{AC,j} \left[G_{AC,ij} \sin\left(\delta_{AC,ij}\right) - B_{AC,ij} \cos\left(\delta_{AC,ij}\right) \right] \tag{22}$$

where $P_{Conv,k}$ and $Q_{Conv,k}$ are the generation of Active and Reactive power ($P_{rect/inv,k}$ and $Q_{rect/inv,k}$) at the converter connecting node k if connected to the VSC. P_{Lk} and Q_{Lk} are the consumption of Active and Reactive power by the Load at node k.

3. Optimal power flow

In case of a large power system, the objective function can be one of the following [2], [5]: a) Minimizing power loss, where P_{gi} is the generation of active power at *i-th* bus and P_{di} is the demand/consumption of active power at *i-th* bus (23), b) Minimizing generation cost, where C_j is the per unit cost function of *j-th* generator and P_{gj} is the generation capacity of *j*-th generator (24), c) Minimizing the deviation of bus voltages at all buses, where $V_{j,m}$ is the measured bus voltage at *j-th* bus and $V_{j,set}$ is the set point voltage at *j-th* bus (Equation 25), d) Maximizing the reactive power supply which can be required under normal or abnormal operating condition of the grid, where $Q_{g,j}$ is the reactive power delivered by the *j-th* generator (26).

$$[MIN]Z = \sum_{i=1}^{n_{bus}} \left(P_{gi} - P_{di}\right) \tag{23}$$

$$[MIN]Z = \sum_{i=1}^{n_g} C_j\left(P_{gj}\right) \tag{24}$$

$$[MIN]Z = \sum_{i=1}^{n_{bus}} \left(V_{j,m} - V_{j,set}\right)^2 \tag{25}$$

$$[MAX]Z = \sum_{i=1}^{n_g} \left(Q_{g,j}\right) \tag{26}$$

In this paper, minimizing transmission loss is considered as the objective function. Based on that, the nonlinear constraints and variables are provided and different optimized solutions are obtained. Interior point algorithm through the Matlab function "*fmincon*", which is efficient in solving constraint nonlinear optimization problems, is used to determine the minima subject to the non-linear constraints and bounded parameters. The decision variables can be a) Active power output of the generating units, b) Generating unit voltages, c) Transformer tap positions, d) Booster transformer phase shifter, e) Operating status of reactive power compensating devices (switched capacitors and reactors), f) Power electronic control variables (HVDC, FACTS). The objective function in this case is the transmission loss (Z). The Inequalities added to determine the OPF solution are as follows.

$$[0.9 \leq V_{AC,DC} \leq 1.1] \tag{27}$$

$$[-0.8 \leq \theta_{AC} \leq 0.2\ ] \tag{28}$$

$$[2\ deg \leq \alpha_{r7}, \gamma_{i8}, \gamma_{i9} \leq 50\ deg] \tag{29}$$

$$[0.6 \leq \cos(\varphi_1, \varphi_2, \varphi_3) \leq 1] \quad (30)$$

4. Case studies

4.1. Description of the hybrid AC/DC system

An example hybrid AC/DC system is chosen for case studies in this paper. The line impedance of each individual line is expressed in Figure 3. The base MVA of the system is assumed as 100 MVA. The shunt admittance of each AC line is assumed as 0.1j. Transformers are shown with turns ratio and impedance value. The converter impedance value is taken as 0.0001 + 0.1643j [16]. The PV-bus information is given for each bus listed in Table 1. To solve the load flow problem, the AC-DC unified algorithm is adopted here.

Table 1. (Bus Data)

Bus Type	Bus Number
Slack Bus	Bus 1
PV Bus	Bus 4, 6
PQ Bus	Bus 2, 3, 5
DC Bus	Bus 7, 8, 9 (converter terminal)

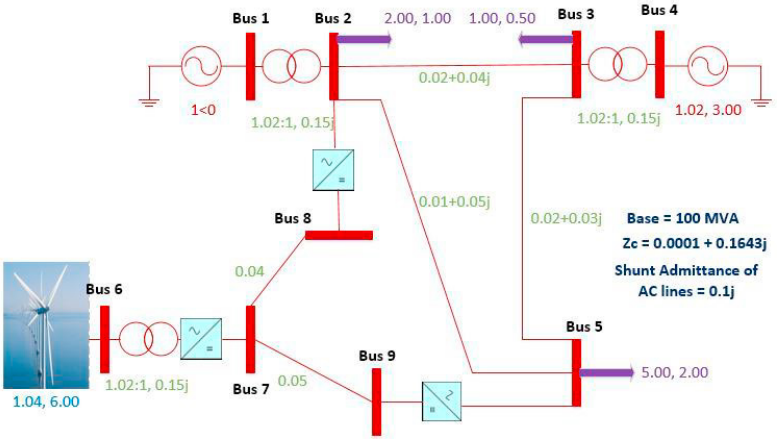

Fig. 3. Multi-terminal hybrid AC/DC network and Offshore Wind Farm

4.2. OPF level A

The optimization function Z is calculated based on the linear & nonlinear constraints and inequalities listed above. From Table 2, it is clear that as the deviations of bus voltage and angles are relaxed the transmission loss decreases gradually by solving the same Optimal Load flow algorithm. With the OPF method applied for case I, II & III, the deviations of voltage magnitudes & angle can be limited by bounding the range (upper/lower); accordingly the objective function value (Transmission Loss) changes.

Table 2 (Results of OPF Level A)

Case	*Control Variables*	*Z (MW)*
I	Bounded, $V = \pm 10\%,\ \theta = \pm 15\%$	11.21
II	Bounded, $V = \pm 10\%,\ \theta = \pm 18\%$	7.58
III	Bounded, $V = \pm 10\%,\ \theta = \pm 20\%$	5.57

4.3. OPF level B

The transmission loss can be further optimized by inserting additional control variables with corresponding upper and lower bounds. In OPF level B, two more cases are chosen as III-a and III-b. Case III is considered as the base case in this level because of its minimum transmission loss with strict voltage and angle deviation limit and is further investigated if the transmission loss can be reduced with additional control variable on top of the base case III. In case of III-a, the firing angles of rectifier and inverter ($\alpha_{rect7}, \gamma_{inv8}, \gamma_{inv9}$) are inserted as additional control variables. In case III-b, the power factor angles of the operating converters ($\varphi_{rect7}, \varphi_{inv8}, \varphi_{inv9}$) in the system are also included as controlled variables with their respective upper and lower bounds. Case III, III-a and III-b are listed in detail in Table 3 with the optimization results.

Table 3. (Results of OPF Level B)

Case	*Control Variables*	*Z (MW)*
III	$[0.9 \leq V_{AC,DC} \leq 1.1],[-0.8 \leq \theta_{AC} \leq 0.2]$	5.57
III-a	$[0.9 \leq V_{AC,DC} \leq 1.1],[-0.8 \leq \theta_{AC} \leq 0.2]$ $[5° \leq \alpha_{rect7}, \gamma_{inv8}, \gamma_{inv9} \leq 45°]$	5.486
III-b	$[0.9 \leq V_{AC,DC} \leq 1.1]$ $[-0.8 \leq \theta_{AC} \leq 0.2]$ $[5° \leq \alpha_{rect7}, \gamma_{inv8}, \gamma_{inv9} \leq 45°]$ $[0.6 \leq \cos(\varphi_{\text{rect7}}, \varphi_{\text{inv8}}, \varphi_{\text{inv9}}) \leq 1]$	5.484

From the Transmission loss values listed in Table 3, it can be safely concluded that the objective function can be further optimized in OPF III-a and OPF III-b. The more the number of controlled variable defined in the optimization process, the better result (value of Z) is expected. But at the same time, it is also interesting to observe that there is a chance of reaching the saturation optimization point beyond which the optimization result may not significantly improve. The saturation effect can be clearly observed by comparing the results in OPF III-a and OPF III-b. Hence, the selection of parameters and specified upper and lower limit for each control variable play the key role in updating the OPF results in each level.

4.4. OPF under different wind scenarios

In this subsection, the OPF study is applied for varying the generation level of the large scale wind park (Low, Medium and High) respectively in three cases. The total Active and Reactive power demand of the system is 800 MW and 350 MVar respectively. In the three scenarios, Wind Turbine Generator (WTG) generation are specified with respective active/reactive power generation as listed in Table 4. The generator outputs of the two conventional generators (G1, G4) connected to Bus1 and Bus 4 are determined by OPF method and listed below. In all three case, the transmission losses of the overall system are minimized.

Table 4. (Results of OPF for Different Wind Production)

WTG production	***WTG Active Power***	***WTG Reactive Power***	***Conventional Gen. (G1) Active Power***	***Conventional Gen. (G1) Reactive Power***	***Conventional Gen. (G4) Active Power***	***Conventional Gen. (G4) Reactive Power***	***Transmission Loss***
Low	200	50	198.82	100.17	250.00	99.36	40.66
Medium	500	150	136.35	94.13	228.17	88.13	12.40
High	700	250	77.47	63.46	122.53	36.54	26.49

It is important to note that, the transmission loss is directly proportional to the distance between the generating units and major load center. From Table 4, it can be observed that the Transmission Loss is minimum in Medium Wind Generation case, because of the resulting distribution of the entire generation capacity between Conventional Generators and Offshore Wind Farm. In case of Low or High Wind generation capacity, bulk power needs to be transmitted to the major load center from distant generating (both Conventional and Offshore Wind) units. In reality, the large-scale power generating units are usually located far from load centers. Hence, it is essential to optimize the

generation capacity and their locations so as to maintain the overall load flow without causing significant transmission losses.

5. Conclusion

The generalized AC/DC model described in this paper offers the scope of implementing a large and complex hybrid system for load flow analysis. Moreover, it is also possible to include the detailed converter model which plays a key role in the multi-terminal AC/DC system. With the control parameters and upper/lower bound of the parameters the model can lead to realistic and optimal solutions.

6. Acknowledgements

The work was supported by both the “Rammeaftale vedrtitrende udnyttelse af PowerlabDK's facillteter” project and the ‘Voltage control on the transmission grid using wind power at other voltage levels (VOLATILE)’ project.

References

[1] “Offshore wind in Europe, Walking the tightrope to success”, March 2015, Ernst & Young et Associés http://www.ewea.org/fileadmin/files/library/publications/reports/EY-Offshore-Wind-in-Europe.pdf [Visited Date: 10.12.2016]
[2] “OFFSHORE WIND VISION” http://offshorewind.works/wp-content/uploads/2015/11/151106_Offshore-Wind-Vision_FINAL.pdf
[3] “European Offshore Supergrid Proposal, Vision and Executive Summary” www. Airtricity.com http://www.trec-uk.org.uk/resources/airtricity_supergrid_V1.4.pdf [Visited Date: 10.12.2016]
[4] “Offshore Wind and the European Supergrid – from vision to reality”, EUFORES, Parliamentary Kick-off 2010, Tilman Schwencke, http://www.eufores.org/fileadmin/eufores/Events/Parliamentary_Events/Offshore_September_2010/EUFORES_Schwencke.pdf
[5] Monica Aragues-Penalba, Jef Beerten, Johan Rimez, Dirk Van Hertem, Oriol Gomis-Bellmunt. “Optimal power flow tool for hybrid AC/DC systems”, proceedings of the 11th Iet International Conference on Ac and Dc Power Transmission, 2015.
[6] H M Mesbah Maruf, Bhaskar Mitra, Prasanth Kumar Sahu, M. Manjrekar, B. H. Chowdhury, “Hybrid High Voltage AC/DC System for Interfacing Off-shore Power Generations with On-Shore Grid”, Proceedings of Ieee Southeastcon — 2016, Volume 2016-, pp. 7506707
[7] Jun Cao, W. Du, H. F. Wang, “An Improved Corrective Security Constrained OPF for Meshed AC/DC Grids with Multi-Terminal VSC-HVDC”, IEEE Transactions on Power Systems, Vol 31, No. 1, January 2016.
[8] F. Akhter, D. E. Macpherson, G. P. Harrison, W. A. Bukhsh, “DC Voltage Droop Control Implementation in the AC/DC Power Flow Algorithm: Combinational Approach”, Proceedings of the 11th Iet International Conference on Ac and Dc Power Transmission, 2015.
[9] Jef Beerten, Stijn Cole, Ronnie Belmans, “Generalized Steady-State VSC MTDC Model for Sequential AC/DC Power Flow Algorithms”, IEEE TRANSACTIONS ON POWER SYSTEMS, VOL. 27, NO. 2, MAY 2012.
[10] Sheng Wang, Jingli Gao, Chuanyue Li, Senthooran Balasubhramaniam, Rui Zheng, Jun Liang, “Coordination of DC power flow controllers and AC/DC converters on optimizing the delivery of wind power”, IET Renewable Power Generation, Vol. 10, Issue 6, July 2016, p. 815 – 823, DOI: 10.1049/iet-rpg.2015.0452.
[11] Monica Aragues-Penalba, Agusti Egea Alvarez, Samuel Galceran Arellano, “Optimal power flow tool for mixed high-voltage alternating current and high-voltage direct current systems for grid integration of large wind power plants”, IET Renewable Power Generation, Vol. 9, Iss. 8, pp. 876–881, 2015.
[12] Qing Li, Mingbo Liu and Huiye Liu, “Piecewise Normalized Normal Constraint Method Applied to Minimization of Voltage Deviation and Active Power Loss in an AC-DC Hybrid Power System”, IEEE TRANSACTIONS ON POWER SYSTEMS, VOL. 30, No. 3, May 2015.
[13] Jef Beerten, Ronnie Belmans, “Development of an open source power flow software for hybrid voltage direct current grids and hybrid AC/DC systems: MATACDC”, IET Generation, Transmission & Distribution, vol. 9, issue 10, pp. 966 - 974.
[14] “Why HVDC”, ABB, http://new.abb.com/systems/hvdc/why-hvdc [Visited: 10.12.2016]
[15] “Technical Advantages of HVDC Transmission”, ABB, [online]http://new.abb.com/systems/hvdc/why-hvdc/technical-advantages [Visited: 10.12.2016]
[16] Jun Cao, Wenjuan Du, Haifeng F. Wang and S. Q. Bu, “Minimization of Transmission Loss in Meshed AC/DC Grids With VSC-MTDC Networks”, IEEE TRANSACTIONS ON POWER SYSTEMS, VOL. 28, NO. 3, AUGUST 2013
[17] J. Beerten, S. Cole, and R. Belmans, “Generalized steady-state VSC MTDC model for sequential AC/DC power flow algorithms,” IEEE Trans. Power Syst., vol. 27, no. 2, pp. 821–829, May 2012.
[18] A Panosyan, B. R. Oswald, “Modified Newton-Raphson Load Flow Analysis For Integrated AC/DC Power Systems”, Upec 2004: 39th International Universitities Power Engineering Conference, Vols 1-3, Conference Proceedings — 2005, pp. 1223-1227
[19] Anish Prasai, Jung-Sik Yim, Deepak Divan, Ashish Bendre and Seung-Ki Sul, “A New Architecture for Offshore Wind Farms”, IEEE Transactions on Power Electronics, Vol. 23, No. 3, May 2008.
[20] A. B. Morton, S. Cowdroy, J. R. A. Hill, M. Halliday, and G. D. Nicholson, “AC or dc economics of grid connection design for offshore wind farms,” in Proc. IEE Int. Conf. AC DC Power Transm., March 2006, pp. 236-240.
[21] N. M. Kirby, X. Lie, M. Luckett, and W. Siepmann, “HVDC transmission for large offshore wind farms,” Power Eng. J., vol. 16, pp. 135–141, Jun. 2002.